Immobilization of Ir(I) complex on covalent triazine frameworks for C—H borylation reactions: A combined experimental and computational study

Norini Tahir [a], Francesco Muniz-Miranda [b], Jonas Everaert [c], Pieter Tack [d], Thomas Heugebaert [c], Karen Leus [a], Laszlo Vincze [d], Christian V. Stevens [c], Veronique Van Speybroeck [b], Pascal Van Der Voort [a,*]

[a] Center for Ordered Materials, Organometallics and Catalysis (COMOC), Department of Chemistry, Ghent University, Krijslaan 281-S3, 9000 Ghent, Belgium
[b] Center for Molecular Modeling (CMM), Ghent University, Technologiepark 903, Zwijnaarde, Belgium
[c] Department of Green Chemistry and Technology, Ghent University, Coupure Links 653, 9000 Ghent, Belgium
[d] X-ray Micro-Spectroscopy and Imaging Group (XMI), Department of Chemistry, Ghent University, Krijslaan 281-S12, 9000 Ghent, Belgium

ARTICLE INFO

ABSTRACT

Metal-modified covalent triazine frameworks (CTFs) have attracted considerable attention in heterogeneous catalysis due to their strong nitrogen-metal interactions exhibiting superior activity, stability and hence recyclability. Herein, we report on a post-metalation of a bipyridine-based CTFs with an Ir (I) complex for C—H borylation of aromatic compounds. Physical characterization of the Ir(I)-based bipyCTF catalyst in combination with density functional theory (DFT) calculations exhibit a high stabilization energy of the Ir-bipy moiety in the frameworks in the presence of B_2Pin_2. By using B_2Pin_2 as a boron source, Ir(I)@bipyCTF efficiently catalyzed the C—H borylation of various aromatic compounds with excellent activity and good recyclability. In addition, XAS analysis of the Ir(I)@bipyCTF gave clear evidence for the coordination environment of the Ir.

1. Introduction

Aromatic boronic acids are highly important compounds that have been used in numerous synthetic procedures [1]. The transition metal-catalyzed C—H borylation of aromatic compounds is the most efficient and convenient synthetic strategy for the synthesis of organoboron compounds. It is a highly economical and environmentally benign process that can be carried out in the absence of a halogenated reactant [2–5]. Among the developed transition metal-based catalysts to date, Ir complexes containing bipyridine-based ligands have shown superior performance exhibiting excellent activity and selectivity for the aromatic C—H borylation under mild reaction conditions [6–8]. In recent decades, intensive research efforts have resulted into the development of Ir-based heterogeneous catalysts for C—H borylation in order to overcome the drawbacks related to homogeneous systems such as difficulties related to the recovery and reuse of the precious Ir catalysts [9]. Various heterogeneous-based bipyridine supports have been developed, including mesoporous silica [10,11], periodic mesoporous organosilica (PMO) [12–14], metal-organic frameworks (MOF) [15–17], and organosilica-nanotubes [18]. These

well-established heterogeneous Ir(I)-based catalysts could catalyze the C—H borylation of arenes exhibiting a high activity and selectivity. However, their durability was somehow hampered and showed a rather low tolerance for the presence of functional groups. For example, the C—H borylation catalyzed by an Ir(I)-based PMO showed a significant decreased catalytic performance during recycling studies [13], whereas for the Ir(I)-based MOF catalysts, the system required high reaction temperatures and long reaction times (up to 72 h) for the C—H borylation of rigid and larger substrates [15].

Within this context, covalent triazine frameworks (CTFs) have recently emerged as potential supports for heterogeneous catalysis due to their high surface area having an abundant nitrogen content [19,20]. CTFs are porous aromatic polymers which consist solely of organic groups connected via strong covalent bonds. CTFs are typically produced through the reversible ionothermal trimerization of polynitriles in molten zinc chloride which acts both as solvent and as catalyst [21–23]. The most exciting feature of CTFs is their flexibility for a specific structural design to control the porosity and functionality, which is of utmost importance towards their use as catalytic support [24]. CTFs also possess superior thermal and chemical stability, hence, exhibiting high resistance to strongly oxidizing and harsh catalytic reaction environments [25].

* Corresponding author.
  E-mail address: pascal.vandervoort@ugent.be (P. Van Der Voort).

Lotsch and co-workers synthesized a functionalized-CTF based on 2,2′-bipyridine building blocks [26]. They demonstrated that this bipyridine-based CTF (later known as bipyCTF) possess specific and strong binding sites for transition metals ions including Co, Ni, Pt, and Pd. Yoon et al. have further investigated the potential of the bipyCTF as a host matrix for metal complexes. They demonstrated that the bipyCTF-functionalized with either an Ir, Rh or Ru complexes exhibited a good catalytic performance in the selective hydrogenation of carbonyl compounds [27–29]. In another study, they explored the incorporation of bimetallic Al-Co in the bipyCTF for the carbonylation of propylene oxide to ß-butyrolactone [30]. These studies clearly demonstrate that the bipyCTF can act as a chelating ligand stabilizing metal complexes for various catalytic applications. In this study, we employed the bipyCTF as catalytic support for the anchoring of the [Ir(OMe)(cod)]$_2$ complex towards the borylation of aromatic C—H bonds. The immobilization of the Ir (I) complex onto the bipyCTF was investigated intensely both experimentally and computationally, showing a high reactivity in the C—H borylation of various arenes and heteroarenes in the presence of B$_2$Pin$_2$ as boron reagent.

2. Experimental section

All chemicals were purchased from commercial suppliers and used without further purification. Nitrogen adsorption analysis was conducted at 77 K using an automated gas sorption system Belsorp-mini II gas analyzer. Prior to sorption measurements, the samples were dried under vacuum at 120 °C overnight to remove adsorbed water. FT-IR spectra in the region of 400–4000 cm^{-1} were recorded on a Thermo Nicolet 6700 FT-IR spectrometer equipped with a nitrogen-cooled MCT detector and a KBr beam splitter. Elemental analysis was measured on a Thermo Scientific Flash 2000 CHNS-O analyzer equipped with a TCD detector. Powder X-ray diffraction (XRPD) patterns were collected on a Thermo Scientific ARL X′Tra diffractometer, operated at 40 kV, 40 mA using Cu-Kα radiation (λ = 1.5406 Å). TGA measurements were performed using a Netzsch STA-449 F3 Jupiter. The samples were heated in the temperature range 30–800 °C under an air atmosphere at a heating rate of 10 °C min^{-1}. The Ir loading was determined using an ICP-OES Optime 8000 atomic emission spectrometer. HAADF-STEM and the EDX mapping analysis was performed using JEOL JEM-2200FS High- Resolution STEM equipped with an EDX spectrometer with a spatial resolution of 0.13 nm, image lens spherical aberration corrector, electron energy loss spectrometer (filter) and an emission field gun (FEG) operating at 200 KeV. X-ray Absorption Spectroscopy (XAS) measurements were performed at beamline BM26A (Dutch-Belgian beamline, DUBBLE) at the ESRF (Grenoble, France) [31]. The conversion of the substrates was identified by a Finnigan Thermo Scientific Trace GC Ultra equipped with an FID, and the yield formation of borylated compounds was determined by means of ^{1}H NMR measurements on a Bruker Advance 300 MHz spectrometer.

2.1. Synthesis of 2,2′-bipyridine-5,5′-dicarbonitrile

The nitrile based monomer was synthesized according to a slightly adopted procedure reported by Duan et al [32]. In first instance, NiCl$_2$·6H$_2$O (0.12 g, 0.5 mmol) was dissolved in 20 mL dry DMF. The resulting mixture was heated to 40 °C and 2-bromo-5-cyanopyridine (1.83 g, 10.0 mmol), anhydrous LiCl (0.43 g, 10.0 mmol) and Zn powder (0.78 g, 12.0 mmol) were added. After raising the temperature to 50 °C, a grain of I$_2$ and two drops of acetic acid were added into the mixture and stirred for 30 min. Afterward, the mixture was cooled down to 0 °C before adding 1 N HCl (15 mL) and stirring it for an additional 30 min.

Hereafter, aqueous ammonia (25%) was added to make the mixture alkaline and the resulting product was extracted with ethyl acetate (3 × 50 mL). The combined organic layers were washed with a 5% aqueous LiCl solution and dried over MgSO$_4$, filtered and concentrated. 2,2′-bipyridine-5,5′-dicarbonitrile was obtained as a pale brown powder in 91% yield (0.94 g). No further purification was required for the next reaction step. ^{1}H NMR (400 MHz, CDCl$_3$): δ 8.97 (2H, dxd, J = 2.0, 0.8 Hz), 8.64 (2H, dxd, J = 8.3, 0.8 Hz), 8.14 (2H, dxd, J = 8.3, 2.1 Hz) (Fig. S1). ^{13}C NMR (100.6 MHz, CDCl$_3$): δ 157.0, 152.1, 140.5, 121.7, 116.5, 110.7 (Fig. S2).

2.2. Synthesis of the bipyCTF

The bipyCTF was synthesized according to the published procedure [26]. Typically, a glass ampoule was charged with 2,2′-bipyridine-5,5′-dicarbonitrile (100 mg, 0.48 mmol) and ZnCl$_2$ (332 mg, 2.40 mmol) in a glove box. The ampoule was flame-sealed under vacuum and heated in an oven towards 400 °C with a heating rate of 100 °C/h and held at this temperature for 48 h. After cooling down to room temperature, the resulting black solid was ground well and stirred in 250 mL of water for 4 h, filtered and washed with water, acetone and refluxed in 250 mL of 1 M HCl overnight, filtered, and washed subsequently with 1 M HCl (3 × 100 mL), H$_2$O (3 × 100 mL), THF (3 × 100 mL), and acetone (3 × 100 mL). The resulting product was dried under vacuum overnight at 150 °C prior to use.

2.3. Post-synthetic metalation of bipyCTF with [Ir(OMe)(cod)]$_2$

To obtain the Ir(I)@bipyCTF catalyst, 140 mg of bipyCTF was added to a solution of [Ir(OMe)(cod)]$_2$ (10.0 mg, 0.015 mmol) in 30 mL anhydrous THF and the mixture was stirred at room temperature. After 24 h, the solid was filtered and washed with THF (3 × 25 mL) to remove the weakly bounded Ir complex and dried under vacuum. It is important to note that all the handlings as mentioned above were done under an inert atmosphere to prevent oxidation of the Ir precursor.

2.4. Computational details

Density functional theory calculations have been performed with the Gaussian 16 suite of programs [33]. Structural optimizations were carried out with the M06 [34] exchange-correlation functional, employing the LanL2DZ combined pseudopotential and basis set [35–37]. The M06 functional is known to yield accurate structural parameters and thermochemical energies with Ir cations [38]. The lack of negative frequencies in relaxed geometries indicate that the optimized structures represent true energy minima. Calculations for the anchoring models shown in Fig. 3 have been carried out including the THF solvent via the polarizable continuum model (PCM) [39]. Calculations for the deprotonation energies have been carried out including the methanol solvent through the PCM procedure. Dispersion interactions have been modelled using the D3 version of Grimme's dispersion with Becke-Johnson damping [40].

2.5. General procedure for the aromatic C—H borylation

All the catalytic tests were carried out in a 25 mL Schlenk-tube which was charged subsequently with bis(pinacolato)diboron (31.75 mg, 0.125 mmol), an arene (0.125 mmol), 3 mL of dry heptane and Ir(I)@bipyCTF (1.5 mol% Ir). The mixture was stirred at 90 °C for 8 h under a nitrogen atmosphere. At the end of the reaction, the reaction mixture was analyzed by means of GC and GC–MS using dodecane as internal standard and the product yield

was determined by ^{1}H NMR using mesitylene as the internal standard.

3. Results and discussion

3.1. Synthesis and characterization

The most commonly applied synthesis method to obtain CTFs is through trimerization of nitrile monomers using $ZnCl_2$ at 400 °C for 40–48 h of reaction [23]. Notably, a high temperature is required to dissolve the monomers in molten $ZnCl_2$ in which Zn^{2+} acts as a Lewis acid catalyst to promote the reversible trimerization throughout the CTF formation. However, at temperatures above 400 °C, carbonization and structural degradation of the triazine ring can occur, whereas shorter reaction times (<40 h) result in an incomplete polymerization [41]. In this study, the bipyCTF was synthesized by heating the 2,2′-bipyridine-5,5′-dicarbonitrile monomer in the presence of $ZnCl_2$ at 400 °C for 48 h, in a vacuum sealed glass ampoule (Scheme 1).

The Fourier Transform Infrared (FT-IR) analysis for the synthesized bipyCTF was performed to evaluate the trimerization process of the framework. The disappearing band of the —CN stretching vibration at 2240 cm^{-1} indicates the complete polymerization of the framework (Fig. S3). Elemental analysis (EA) revealed an increase in the C/N ratio of the bipyCTF in comparison to the theoretically calculated values due to the decomposition of nitrile building blocks and the partial carbonization of the frameworks during the synthesis reaction, which is commonly observed feature for CTFs (Table S1) [42]. Furthermore, the Powder X-ray diffraction (PXRD) measurement shows a broad diffraction peak representing the structural ordering of the bipyCTF (Fig. S4) [43]. The thermal stability of the studied bipyCTF was examined by means of Thermogravimetric analysis (TGA) demonstrating that the bipyCTF material starts to decompose at 450 °C, whereas approximately 10% of weight loss below 100 °C can be assigned to adsorbed CO_2 or solvents (Fig. S5). However, before the catalytic test, the samples were preheated overnight at 150 °C in vacuo, which should remove all adsorbed species.

The Ir(I)bipyCTF was prepared by post-metalation of the synthesized bipyCTF with [Ir(OMe)(cod)]$_2$ in THF at room temperature, as shown in Scheme 1. ICP-OES analysis was performed to determine the metal loading which amounts 8.26 wt% Ir

(0.43 mmol g^{-1}) (Table S2). The nitrogen adsorption isotherms of both the bipyCTF and Ir(I)bipyCTF material were subsequently recorded at 77 K to determine the porosity of the networks. As shown in Fig. 1, both materials exhibit a typical type I isotherms which is characterized by a sharp N_2 uptakes at low relative pressure. The Brunauer-Emmett-Teller (BET) surface area and pore volume of the bipyCTF are calculated to be 714 m^2 g^{-1} and 0.39 cm^3 g^{-1}, respectively. These values decreased after the coordination of the Ir obtaining 494 m^2 g^{-1} and 0.27 cm^3 g^{-1} for the BET surface area and total pore volume, respectively (Table S2). To evaluate the occupancy of Ir(I) complex inside the pore system of the bipyCTF, we have calculated the theoretical occupied volume and weight based on a 0.43 mmol g^{-1} Ir-complex loading which amounts 0.043 cm^3 g^{-1} and 142 mg g^{-1}, respectively. Starting from the pore volume of the pristine bipyCTF being 0.39 cm^3 g^{-1}, and taking into account only the weight increase, the theoretical pore volume of the catalyst with all complexes on the outside would become 0.34 cm^3 g^{-1}. The occupied volume by the complex amounts 0.043 cm^3 g^{-1}, the theoretical pore volume considering all complexes inside the pores is then 0.29 cm^3 g^{-1}, which is slightly higher than the experimental pore volume (0.27 cm^3 g^{-1}), but definitely lower than 0.34 cm^3 g^{-1}, which would be obtained taking only the weight increase and not any pore filling into account. These data are a good indication that most of the complexes are inside the pores. The presence of the anchored Ir in the Ir(I)@bipyCTF material was further confirmed by high angle annular dark field scanning transmission electron microscopy (HAADF-STEM) and the corresponding energy dispersive X-ray spectroscopy (EDX) mapping images (Fig. S6). The main elements, namely carbon and nitrogen are well dispersed and the Ir(I) complex was uniformly distributed throughout the frameworks.

3.2. Theoretical calculations

Density functional theory (DFT) calculations have been performed to investigate the anchoring of the Ir(I) complex onto the bipyCTFs (see Section 2.4 for the complete computational details). Various anchoring models were studied including the possibility of deprotonation of bipy with the methoxy anion ($^-$OCH$_3$). This process can not a priori be ruled out because: (i) the $^-$OCH$_3$ anion, which has strong basic properties, is present in the [Ir(OMe)(cod)]$_2$ precursors complex; (ii) the C—H ionic dissociation
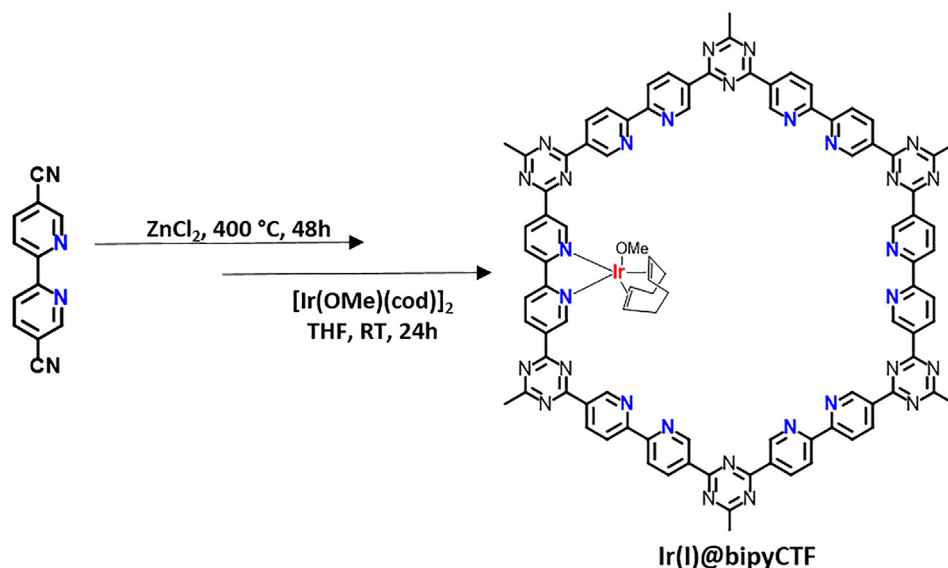
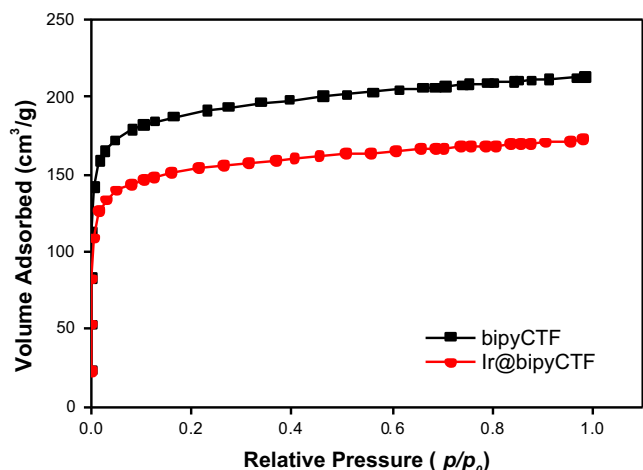**Scheme 1.** Schematic representation of the synthesis of Ir(I)@bipyCTF.

Fig. 1. Nitrogen adsorption isotherms of bipyCTF (black) and Ir(I)@bipyCTF (red) measured at 77 K. (For interpretation of the references to colour in this figure legend, the reader is referred to the web version of this article.)

energies of the bipy embedded into CTF are close to the O—H ionic dissociation energy of methanol (Fig. S7). In fact, regarding point (ii), an increase in the acidity of bipy was observed when it is embedded into the CTF environment. This increase has been traced back to the effect of the nearby triazine residues, as shown in Fig. S7, which makes the C—H bond in bipy less covalent and more prone to deprotonation.

Various anchoring models have been considered which are shown in Fig. 2, along with their stabilization free energy. Model 1 considers an anchoring of a $^-OCH_3$ anion to the two N atoms of bipy, whereas in models 2 and 3 the anchoring is through one N atom (of triazine in model 2, of bipy in model 3) and one deprotonated C atom of bipy, whereas methanol is basically dissociated from the Ir(I) cation. To assess the stability of the various model

compounds, their relative energies have been computed in respect to their subunits (namely the triazine-bipy-triazine unit, Ir(I)-cod, and $^-OCH_3$/methanol), according to the following equation:

$$\Delta G = G[model] - G[Ir(I)\text{-}cod] - G[^-OCH_3/methanol] - G[protonated/deprotonated triazine - bpy - triazine]$$

This equation can be used because the three models have the same number of atoms overall and the same charge (namely, zero), even if their own subunits differ regarding this characteristic (for example, the methoxy anion has a negative charge and one proton less than methanol). The energies are reported in Fig. 2. The ΔG reported in the previous equation is referred to the constituents of a specific model, whose details are reported in the Supporting Information.

These data show that model 1 has the highest stabilization energy; however, model 3 has a similar stabilization energy and thus cannot be ruled out in principle. Hence, two further model complexes were considered to study the possible coordination with B_2Pin_2.

In fact, after addition of B_2Pin_2, the Ir complex would be compound A.2 if no deprotonation of the bipy ring occurs ("anchoring A"), whereas it would lead to complex B.2 if bipy is really deprotonated and Ir is anchored to a C^- anion ("anchoring B") (Fig. 3). Model A.2 and B.2 involve coordination with three and two BPin units, as their precursor compounds A.1 and B.1 had three and two coordination bonds with the non-CTF ligands. Models A.2 and B.2 have the same charge but a different number of atoms, so to compare their relative stability it is not possible to just straightforwardly subtract the free energy of their constituent subunits from their own energy. In fact, to compare their relative energy we considered the following formal reaction connecting the two complexes A.2 and B.2:
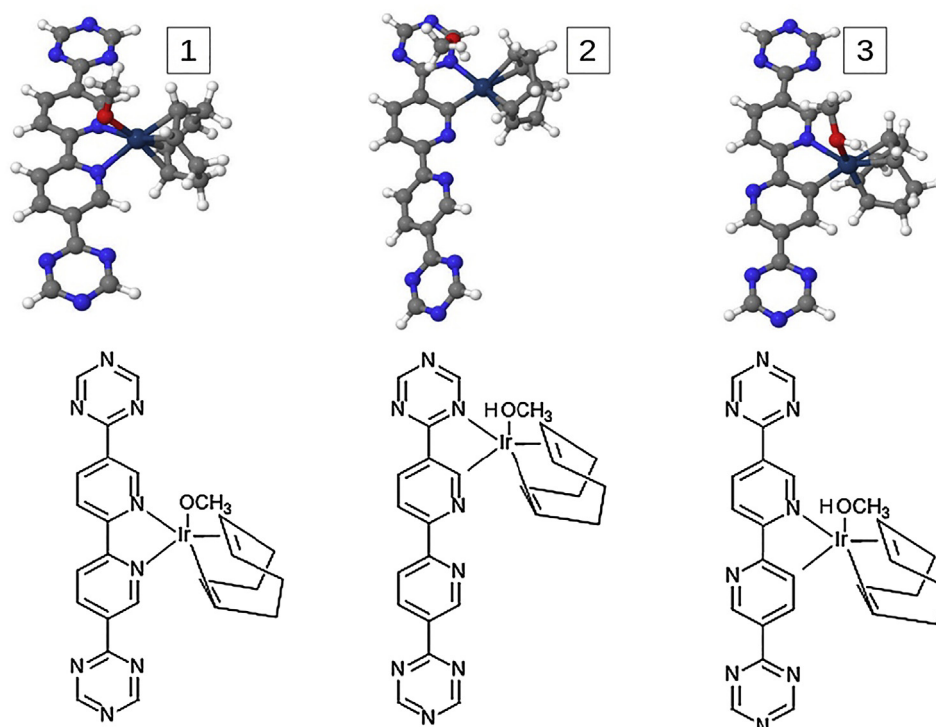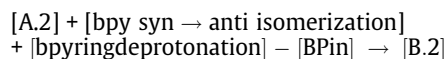
$$[A.2] + [bpy\ syn \rightarrow anti\ isomerization] + [bpy\ ring\ deprotonation] - [BPin] \rightarrow [B.2]$$

Fig. 2. Structurally relaxed anchoring models (upper row) and their schematic formula (lower row). The stabilization energies are −444 kJ/mol (model 1), −414 kJ/mol (model 2), −439 kJ/mol (model 3).
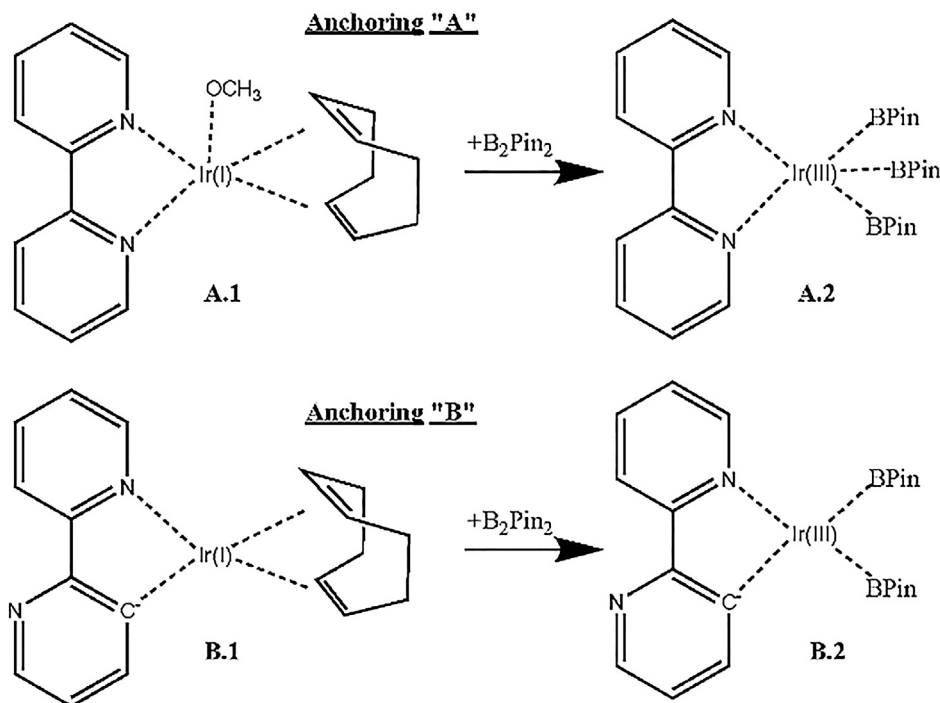
Fig. 3. Possible intermediate Ir(III) complexes formation after treatment with B₂Pin₂. Optimized structures are reported in Fig. S8 of the Supporting Information.

Thus, in this case we have computed the free energy difference $\Delta G = G_{products} - G_{reagents}$ for this formal reaction as:

$$\Delta G = G_{products} - G_{reagents} = G[B.2] - G[A.2] - G[bpy\ syn \rightarrow antiisomerization] - G[bpydeprotonation] + G[BPin]$$

We found that in this case $\Delta G = +106$ kJ/mole (see the details in the Supplementary Information), thus indicating that the B.2 complex (with Ir anchored to a deprotonated bipy ring) is significantly less stable than complex A.2 (with Ir anchored to the two N atoms of bipy). As a consequence, these calculations suggest that the Ir(I) complex is indeed anchored to the CTF framework through the two N atoms of bipy and that this compound would be the actual active complex for the catalysis cycle.

3.3. Aromatic C—H borylation catalyzed by Ir(I)@bipyCTF

The catalytic performance of the Ir(I)@bipyCTF was evaluated for the C—H borylation of arenes and heteroarenes under mild reaction conditions. Initially, the arene 1,2-dichlorobenzene (2 equiv.) was examined in the presence of B₂Pin₂ (1 equiv.) at 70 °C for 24 h using Ir(I)@bipyCTF (1.5 mol% Ir) as catalyst in various solvents. The results are summarized in Table 1. No borylated products were observed when the borylation reaction was conducted in polar solvents such as THF and DMF (Table 1, Entry 1 and 2). However, 18% yield was obtained in heptane at 70 °C (Table 1, Entry 3). The obtained results are in accordance to literature demonstrating that the solvent polarity has a substantial effect on the conversion of the substrate [11,44]. When the reaction temperature was increased to 90 °C, the yield significantly rose to 70% (Table 1, Entry 4). The amount of the boron reagent also plays a crucial role in the yield of the product [45]. For instance, upon increasing of one equivalent of B₂Pin₂, the rate of the borylation reaction increases drastically, reaching 95% yield after 8 h of reaction (Table 1, Entry 5).

Several control experiments were performed. The borylation of 1,2-dichlorobenzene catalyzed by [Ir(OMe)(cod)]₂ and bipyCTF,

Table 1
Ir(I)@bipyCTF catalyzed C—H borylation of 1,2-dichlorobenzene.[a]
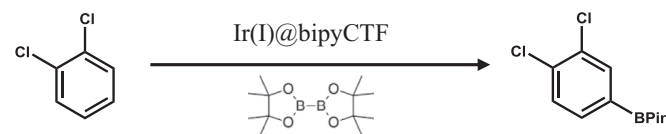
Entry	DCB:B₂Pin₂[b]	Solvent	T (°C)	Time (h)	Yield (%)[c]
1	1:0.5	THF	70	24	0
2	1:0.5	DMF	70	24	0
3	1:0.5	Heptane	70	24	18
4	1:0.5	Heptane	90	24	70
5	1:1	Heptane	90	8	95

[a] Reaction conditions: Ir(I)@bipyCTF (1.5 mol% Ir), 1,2-dichlorobenzene, B₂Pin₂, dodecane (1 mmol).
[b] Substrate to boron reagent mol ratio.
[c] Yield was determined by ¹H NMR.

separately, were carried out under the optimized reaction conditions (Table 2, Entry 2 and 3). Apparently, no catalytic activity was observed in both control experiments. In another control test, the bipyCTF and the [Ir(OMe)(cod)]₂ were added together resulting in a poor yield of only 10% after an extended reaction time of 24 h (Table 2, Entry 4). This demonstrates that the Ir(I) complex can catalyze the C—H borylation reaction in the presence of a bipy-based support. Nevertheless, only when the Ir(I) complex is anchored onto the bipyCTF, a high product yield of 95% was obtained after 8 h of reaction (Table 2, Entry 1). Additionally, the Ir(I)@bipyCTF catalyst exhibited an initial slower reactivity compared to its homogeneous analog, as can be seen in the kinetic profiles for both catalysts (see Fig. 4).

We extended the scope of substrates using various arenes and heteroarenes having electron-withdrawing and electron-donating groups under the optimized catalytic reaction conditions. In general, the Ir(I)@bipyCTF was able to catalyze the C—H borylation

Table 2
Control experiments C—H borylation of 1,2-dichlorobenzene.[a]

Entry	Catalyst	Yield (%)[b]	TON
1	Ir(I)@bipyCTF	95	64
2	[Ir(OMe)(cod)]$_2$	0	0
3	bipyCTF	0	0
4	[Ir(OMe)(cod)]$_2$ + bipyCTF	10[c]	8

[a] Reaction conditions: Ir(I)@bipyCTF (1.5 mol% Ir), 1,2-dichlorobenzene (1 equiv.), B$_2$Pin$_2$ (1 equiv.), 90 °C, heptane, 8 h.
[b] Yield was determined by ^{1}H NMR.
[c] Yield obtained after 24 h of reaction.

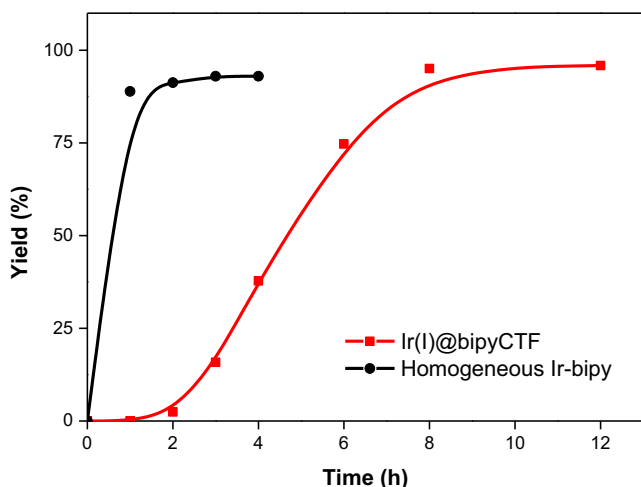**Fig. 4.** Kinetic profiles for the C—H borylation of 1,2-dichlorobenzene catalyzed by Ir(I)@bipyCTF and its homogeneous counterpart.

Table 3
C—H borylation of arenes and heteroarenes catalyzed by Ir(I)@bipyCTF.[a]

Entry	Substrate	Product	Yield (%)[b]
1			95
2			78
3			56
4			92
5			84

[a] Reaction conditions: Ir(I)@bipyCTF (1.5 mol% Ir), arene (1 equiv.), B$_2$Pin$_2$ (1 equiv.), 90 °C, heptane, 8 h.
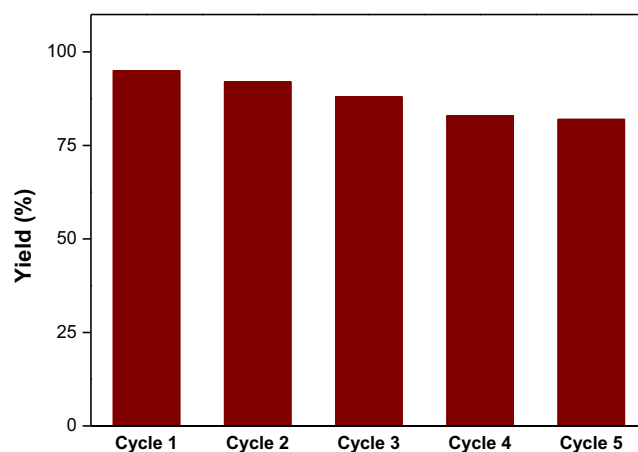[b] Yield was determined by ^{1}H NMR.

Fig. 5. Reusability of the Ir(I)@bipyCTF catalyst for C—H borylation of 1,2-dichlorobenzene.

of various substrates and afforded good to excellent yield of the corresponding borylated products, as summarized in Table 3. The obtained results were in accordance with the literature, demonstrating that the Ir catalyst favors the conversion of electron-poor arenes in the C—H borylation [46,47]. For example, it can be seen that for the borylation of 3- bromobenzotrifluoride, a higher catalytic activity was observed in comparison to 3-(trifluoromethyl) anisole using similar reaction conditions, for which a yield of 78% and 56%, respectively was obtained (Table 3, Entry 2 and 3). Moreover, the regioselectivity of the borylation of arenes was controlled by the steric effects, which means that the C—H boryation occurs at the least sterically accessible C—H position of the arene. On the other hand, the borylation of the heteroarenes is mainly determined by electronic effects which preferentially takes place at the C—H bond α-to the heteroatom [48]. As can be seen from Table 2 (Entry 4 and 5), the borylation of indole and pyrrole, gives 92% and 84% of the respective borylated products.

A hot filtration test was conducted to verify the heterogeneous nature of the catalytic process. After the removal of the catalyst by means of filtration, the catalyst-free reaction solution was stirred for an additional 8 h (Fig. S9). No catalytic activity was observed in the absence of the catalyst, which subsequently demonstrates the heterogeneity of the Ir(I)@bipyCTF catalyst in nature. As for the recycling tests, after the first cycle, the catalyst was recovered by filtration, washed thoroughly with heptane and dried under vacuum. The performance of the recycled catalyst in the borylation of 1,2-dichlorobenzene up to five successive runs is shown in Fig. 5. Only a slight loss of product yield was observed during the sequential tests. This loss in product yield is probably due to the loss of some catalyst during the recovery process. The ICP-OES analysis, performed after the first catalytic run, showed the presence of 8.09 wt% amount of Ir suggesting no significant leaching of the Ir complex during the course of the reaction.

In addition, a comparison has been made between our Ir(I) @bipyCTF catalyst to the other reported heterogeneous Ir(I)-based catalysts (Table 4). Although a one-on-one comparison with the PMO-based support catalyst by Inagaki *et al.* [13] and the MOF-based support variant by Lin *et al.* [15] is not straightforward, due to different operating conditions, we can conclude that the Ir(I) @bipyCTF is a highly efficient catalyst. It adds to the high activity also the larger pores (MOFs) and a very high stability.

An Ir-L$_3$ edge XANES investigation of the Ir(I)@bipyCTF catalyst before and after a catalytic run was carried out to elucidate the coordination environment of the Ir center in the catalytic system.

Table 4
Heterogeneous Ir-based catalysts catalyzed C—H borylation of 1,2-dichlorobenzene.

Catalyst	Reaction conditions	TON	Yield (%)	Ref.
Ir(I)@bipyCTF	1.5 mol% Ir/90 °C/heptane/8 h	64	95	This study
Ir(cod)-BPy$_{0.3}$-NT	1.5 mol% Ir/80 °C/12 h	64	97	[18]
Ir-Bpy-PMO	0.75 mol% Ir/80 °C/cyclohexane/12 h	34*	92	[13,14]
bpy-UiO-Ir	3.0 mol% Ir/115 °C/heptane/72 h	NR	93	[15,17]
Ir-bpy-SBA-15	1.5 mol% Ir/70 °C/hexane/48 h	136	95	[11]

* TON was calculated for using benzene as substrate.
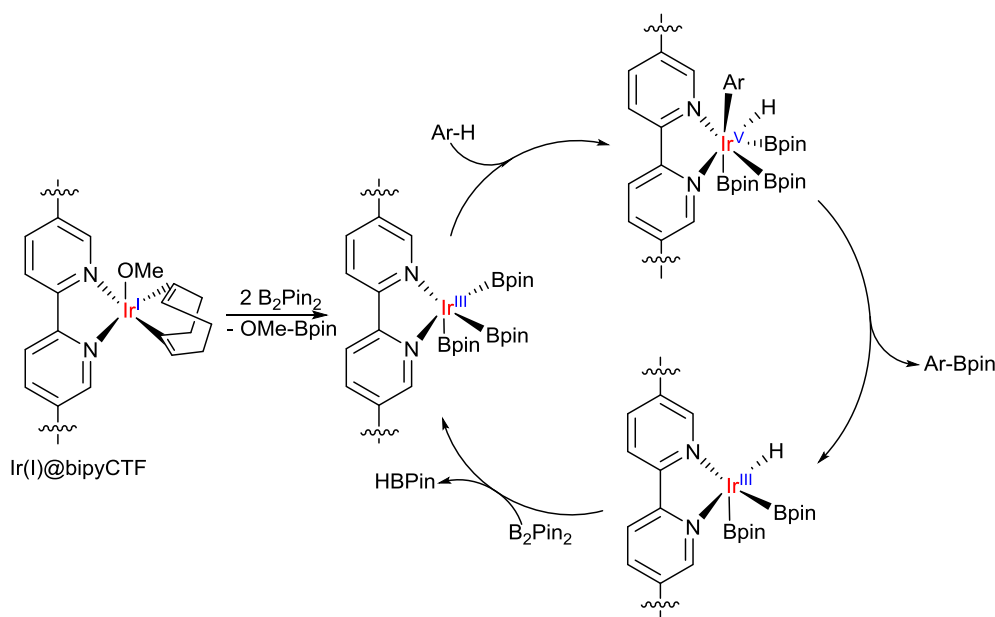
Scheme 2. A proposed plausible mechanism for C—H borylation of arene catalyzed by Ir(I)@bipyCTF [46].

The measurement displays a clear increase in the white line intensity (11.22 keV) for the sample after catalysis (Fig. S10). This white line corresponds to a 2p → 5d electron transition. As the white line intensity increases, the 5d electron density decreases, denoting a shift from Ir(I) to Ir(III). This occasion can be explained by the catalytic reaction mechanism proposed by Hartwig and Miyaura's (Scheme 2) [46]. During the catalytic reaction, an Ir(III) complex is formed by the reaction of an Ir(I) complex with B$_2$pin$_2$. As the reaction progresses, the active intermediate Ir(III) complex will regenerate by the consumption of B$_2$pin$_2$, explaining the increase in white line intensity. In-situ XANES experiments were also performed to monitor the change in Ir state as the catalytic reaction progresses (Fig. S11). A gradual increase in white line intensity can be perceived, corresponding to a gradual increase in the presence of Ir(III)@bipyCTF. These results are in agreement with the theoretical aforementioned earlier in this study stating that the Ir state changes due to a decrease in B$_2$Pin$_2$ as the reaction progresses.

4. Conclusions

The straightforward post-synthetic metalation of bipyCTF with [Ir(OMe)(cod)]$_2$ afforded a robust and efficient heterogeneous system for borylation of aromatic C—H bonds. Ir(I)@bipyCTF exhibited excellent catalytic activity for borylation of arenes and heteroarenes using B$_2$Pin$_2$ as the borylating agent. The DFT calculations gave strong evidence for Ir(I)@bipyCTF anchoring and elucidated its local geometry, while XAS analysis confirmed the change of the Ir state in the catalyst which has a similar environment to that of

the homogeneous counterpart. The heterogeneity test revealed the stability and reusability of the developed heterogeneous-based bipyCTF catalyst for at least five cycles without significant loss of activity. More importantly, the catalyst performs effectively under mild reaction conditions and tolerance to functional groups which showed a similar trend to the typical homogeneous iridium-based catalysts and displayed better performances than the conventional iridium-based heterogeneous catalysts.

Author contributions

N. Tahir synthesized, analyzed the catalyst and performed the catalytic reactions under the supervision of P. Van Der Voort. J. Everaert and T. Heugebaert synthesized the monomer under the supervision of C. V. Stevens. P. Tack and K. Leus performed the XAS analysis under the supervision of L. Vincze. F. Muniz-Miranda performed the theoretical calculations under the supervision of V. Van Speybroeck. N. Tahir wrote the draft initial paper while F. Muniz-Miranda contributed the theoretical calculations section and P. Tack contributed the XAS analysis section. All authors contributed to revising the paper and have given approval to the final version of the manuscript.

Notes: The authors declare no competing interest.

Acknowledgment

Appendix A. Supplementary material

Supplementary data to this article can be found online at https://doi.org/10.1016/j.jcat.2019.01.030.

References

[1] L. Xu, Decarboxylative borylation: new avenues for the preparation of organoboron compounds, Eur. J. Org. Chem. 2018 (2018) 3884–3890.
[2] T. Gensch, M.N. Hopkinson, F. Glorius, J. Wencel-Delord, Mild metal-catalyzed C-H activation: examples and concepts, Chem. Soc. Rev. 45 (2016) 2900–2936.
[3] I.A.I. Mkhalid, J.H. Barnard, T.B. Marder, J.M. Murphy, J.F. Hartwig, C−H activation for the construction of C−B bonds, Chem. Rev. 110 (2010) 890–931.
[4] W.K. Chow, O.Y. Yuen, P.Y. Choy, C.M. So, C.P. Lau, W.T. Wong, F.Y. Kwong, A decade advancement of transition metal-catalyzed borylation of aryl halides and sulfonates, RSC Adv. 3 (2013) 12518–12539.
[5] J.F. Hartwig, Borylation and silylation of C-H bonds: a platform for diverse C-H bond functionalizations, Acc. Chem. Res. 45 (2012) 864–873.
[6] E. Fernández, A.M. Segarra, Iridium-catalyzed boron-addition, in: Iridium Complexes in Organic Synthesis, Wiley-VCH Verlag GmbH & Co. KGaA, 2009, pp. 173–194.
[7] V.A. Kallepalli, Iridium Catalyzed C-H Activation/borylation of Aromatic/ heteroaromatic Substrates and Its Application in Small Molecule Synthesis, 2010.
[8] T. Ishiyama, J. Takagi, K. Ishida, N. Miyaura, N.R. Anastasi, J.F. Hartwig, Mild iridium-catalyzed borylation of arenes. High turnover numbers, room temperature reactions, and isolation of a potential intermediate, J. Am. Chem. Soc. 124 (2002) 390–391.
[9] S. Santoro, S.I. Kozhushkov, L. Ackermann, L. Vaccaro, Heterogeneous catalytic approaches in C-H activation reactions, Green Chem. 18 (2016) 3471–3493.
[10] S. Kawamorita, H. Ohmiya, K. Hara, A. Fukuoka, M. Sawamura, Directed ortho borylation of functionalized arenes catalyzed by a silica-supported compact phosphine−iridium system, J. Am. Chem. Soc. 131 (2009) 5058–5059.
[11] F. Wu, Y. Feng, C.W. Jones, Recyclable silica-supported iridium bipyridine catalyst for aromatic C-H borylation, ACS Catal. 4 (2014) 1365–1375.
[12] W.R. Grüning, G. Siddiqi, O.V. Safonova, C. Copéret, Bipyridine periodic mesoporous organosilica: a solid ligand for the iridium-catalyzed borylation of C H bonds, Adv. Synth. Catal. 356 (2014) 673–679.
[13] M. Waki, Y. Maegawa, K. Hara, Y. Goto, S. Shirai, Y. Yamada, N. Mizoshita, T. Tani, W.-J. Chun, S. Muratsugu, M. Tada, A. Fukuoka, S. Inagaki, A solid chelating ligand: periodic mesoporous organosilica containing 2,2′-bipyridine within the pore walls, J. Am. Chem. Soc. 136 (2014) 4003–4011.
[14] Y. Maegawa, S. Inagaki, Iridium-bipyridine periodic mesoporous organosilica catalyzed direct C-H borylation using a pinacolborane, Dalton Trans. 44 (2015) 13007–13016.
[15] K. Manna, T. Zhang, W. Lin, Postsynthetic metalation of bipyridyl-containing metal-organic frameworks for highly efficient catalytic organic transformations, J. Am. Chem. Soc. 136 (2014) 6566–6569.
[16] M.I. Gonzalez, E.D. Bloch, J.A. Mason, S.J. Teat, J.R. Long, Single-crystal-to-single-crystal metalation of a metal-organic framework: a route toward structurally well-defined catalysts, Inorg. Chem. 54 (2015) 2995–3005.
[17] K. Manna, T. Zhang, F.X. Greene, W. Lin, Bipyridine- and phenanthroline-based metal-organic frameworks for highly efficient and tandem catalytic organic transformations via directed C-H Activation, J. Am. Chem. Soc. 137 (2015) 2665–2673.
[18] S. Zhang, H. Wang, M. Li, J. Han, X. Liu, J. Gong, Molecular heterogeneous catalysts derived from bipyridine-based organosilica nanotubes for C-H bond activation, Chem. Sci. 8 (2017) 4489–4496.
[19] S.M.J. Rogge, A. Bavykina, J. Hajek, H. Garcia, A.I. Olivos-Suarez, A. Sepulveda-Escribano, A. Vimont, G. Clet, P. Bazin, F. Kapteijn, M. Daturi, E.V. Ramos-Fernandez, F.X. Llabres i Xamena, V. Van Speybroeck, J. Gascon, Metal-organic and covalent organic frameworks as single-site catalysts, Chem. Soc. Rev. 46 (2017) 3134–3184.
[20] P. Puthiaraj, Y.-R. Lee, S. Zhang, W.-S. Ahn, Triazine-based covalent organic polymers: design, synthesis and applications in heterogeneous catalysis, J. Mater. Chem. A 4 (2016) 16288–16311.

[21] X. Feng, X. Ding, D. Jiang, Covalent organic frameworks, Chem. Soc. Rev. 41 (2012) 6010–6022.
[22] S.-Y. Ding, W. Wang, Covalent organic frameworks (COFs): from design to applications, Chem. Soc. Rev. 42 (2013) 548–568.
[23] P. Kuhn, M. Antonietti, A. Thomas, Porous, covalent triazine-based frameworks prepared by ionothermal synthesis, Angew. Chem. Int. Ed. Engl. 47 (2008) 3450–3453.
[24] J. Artz, Covalent triazine-based frameworks—tailor-made catalysts and catalyst supports for molecular and nanoparticulate species, ChemCatChem 10 (2018) 1753–1771.
[25] J. Artz, S. Mallmann, R. Palkovits, Selective aerobic oxidation of HMF to 2,5-diformylfuran on covalent triazine frameworks-supported Ru catalysts, ChemSusChem 8 (2015) 672–679.
[26] S. Hug, M.E. Tauchert, S. Li, U.E. Pachmayr, B.V. Lotsch, A functional triazine framework based on N-heterocyclic building blocks, J. Mater. Chem. 22 (2012) 13956–13964.
[27] K. Park, G.H. Gunasekar, N. Prakash, K.-D. Jung, S. Yoon, A highly efficient heterogenized iridium complex for the catalytic hydrogenation of carbon dioxide to formate, ChemSusChem 8 (2015) 3410–3413.
[28] P. Sudakar, G.H. Gunasekar, I.H. Baek, S. Yoon, Recyclable and efficient heterogenized Rh and Ir catalysts for the transfer hydrogenation of carbonyl compounds in aqueous medium, Green Chem. 18 (2016) 6456–6461.
[29] G.H. Gunasekar, J. Shin, K.-D. Jung, K. Park, S. Yoon, Design strategy toward recyclable and highly efficient heterogeneous catalysts for the hydrogenation of CO2 to formate, ACS Catal. 8 (2018) 4346–4353.
[30] S. Rajendiran, P. Natarajan, S. Yoon, A covalent triazine framework-based heterogenized Al-Co bimetallic catalyst for the ring-expansion carbonylation of epoxide to [small beta]-lactone, RSC Adv. 7 (2017) 4635–4638.
[31] S. Nikitenko, A.M. Beale, A.M.J. van der Eerden, S.D.M. Jacques, O. Leynaud, M. G. O'Brien, D. Detollenaere, R. Kaptein, B.M. Weckhuysen, W. Bras, Implementation of a combined SAXS/WAXS/QEXAFS set-up for time-resolved in situ experiments, J. Synchrotron Radiat. 15 (2008) 632–640.
[32] L.-Y. Liao, X.-R. Kong, X.-F. Duan, Reductive couplings of 2-halopyridines without external ligand: phosphine-free nickel-catalyzed synthesis of symmetrical and unsymmetrical 2,2′-bipyridines, J. Org. Chem. 79 (2014) 777–782.
[33] M.J. Frisch, G.W. Trucks, H.B. Schlegel, G.E. Scuseria, M.A. Robb, J.R. Cheeseman, G. Scalmani, V. Barone, G.A. Petersson, H. Nakatsuji, X. Li, M. Caricato, A.V. Marenich, J. Bloino, B.G. Janesko, R. Gomperts, B. Mennucci, H.P. Hratchian, J.V. Ortiz, A.F. Izmaylov, J.L. Sonnenberg, Williams, F. Ding, F. Lipparini, F. Egidi, J. Goings, B. Peng, A. Petrone, T. Henderson, D. Ranasinghe, V.G. Zakrzewski, J. Gao, N. Rega, G. Zheng, W. Liang, M. Hada, M. Ehara, K. Toyota, R. Fukuda, J. Hasegawa, M. Ishida, T. Nakajima, Y. Honda, O. Kitao, H. Nakai, T. Vreven, K. Throssell, J.A. Montgomery Jr., J.E. Peralta, F. Ogliaro, M.J. Bearpark, J.J. Heyd, E. N. Brothers, K.N. Kudin, V.N. Staroverov, T.A. Keith, R. Kobayashi, J. Normand, K. Raghavachari, A.P. Rendell, J.C. Burant, S.S. Iyengar, J. Tomasi, M. Cossi, J.M. Millam, M. Klene, C. Adamo, R. Cammi, J.W. Ochterski, R.L. Martin, K. Morokuma, O. Farkas, J.B. Foresman, D.J. Fox, Gaussian 16 Rev. B.01, in, Wallingford, CT, 2016.
[34] Y. Zhao, D.G. Truhlar, The M06 suite of density functionals for main group thermochemistry, thermochemical kinetics, noncovalent interactions, excited states, and transition elements: two new functionals and systematic testing of four M06-class functionals and 12 other functionals, Theor. Chem. Acc. 120 (2008) 215–241.
[35] P.J. Hay, W.R. Wadt, Ab initio effective core potentials for molecular calculations. Potentials for K to Au including the outermost core orbitals, J. Chem. Phys. 82 (1985) 299–310.
[36] W.R. Wadt, P.J. Hay, Ab initio effective core potentials for molecular calculations. Potentials for main group elements Na to Bi, J. Chem. Phys. 82 (1985) 284–298.
[37] P.J. Hay, W.R. Wadt, Ab initio effective core potentials for molecular calculations. Potentials for the transition metal atoms Sc to Hg, J. Chem. Phys. 82 (1985) 270–283.
[38] D.-D. Zhang, X.-K. Chen, H.-L. Liu, X.-R. Huang, DFT study on the iridium-catalyzed multi-alkylation of alcohol with ammonia, RSC Adv. 6 (2016) 87362–87372.
[39] J. Tomasi, B. Mennucci, R. Cammi, Quantum mechanical continuum solvation models, Chem. Rev. 105 (2005) 2999–3094.
[40] S. Grimme, S. Ehrlich, L. Goerigk, Effect of the damping function in dispersion corrected density functional theory, J. Comput. Chem. 32 (2011) 1456–1465.
[41] P. Kuhn, A. Forget, D. Su, A. Thomas, M. Antonietti, From microporous regular frameworks to mesoporous materials with ultrahigh surface area: dynamic reorganization of porous polymer networks, J. Am. Chem. Soc. 130 (2008) 13333–13337.
[42] P. Kuhn, A. Thomas, M. Antonietti, Toward tailorable porous organic polymer networks: a high-temperature dynamic polymerization scheme based on aromatic nitriles, Macromolecules 42 (2009) 319–326.
[43] S. Ren, M.J. Bojdys, R. Dawson, A. Laybourn, Y.Z. Khimyak, D.J. Adams, A.I. Cooper, Porous, fluorescent, covalent triazine-based frameworks via room-temperature and microwave-assisted synthesis, Adv. Mater. 24 (2012) 2357–2361.

[44] T. Ishiyama, J. Takagi, J.F. Hartwig, N. Miyaura, A stoichiometric aromatic C H borylation catalyzed by iridium(I)/2,2′-bipyridine complexes at room temperature, Angew. Chem. Int. Ed. 41 (2002) 3056–3058.

[45] D.N. Coventry, A.S. Batsanov, A.E. Goeta, J.A.K. Howard, T.B. Marder, R.N. Perutz, Selective Ir-catalysed borylation of polycyclic aromatic hydrocarbons: structures of naphthalene-2,6-bis(boronate), pyrene-2,7-bis(boronate) and perylene-2,5,8,11-tetra(boronate) esters, Chem. Commun. (2005) 2172–2174.

[46] T.M. Boller, J.M. Murphy, M. Hapke, T. Ishiyama, N. Miyaura, J.F. Hartwig, Mechanism of the mild functionalization of arenes by diboron reagents catalyzed by iridium complexes. Intermediacy and chemistry of bipyridine-ligated iridium trisboryl complexes, J. Am. Chem. Soc. 127 (2005) 14263–14278.

[47] J.F. Hartwig, Regioselectivity of the borylation of alkanes and arenes, Chem. Soc. Rev. 40 (2011) 1992–2002.

[48] C. Haldar, M. Emdadul Hoque, R. Bisht, B. Chattopadhyay, Concept of Ir-catalyzed CH bond activation/borylation by noncovalent interaction, Tetrahedron Lett. 59 (2018) 1269–1277.